0026-895X/09/7604-766–777$20.00
MOLECULAR PHARMACOLOGY
Copyright © 2009 The American Society for Pharmacology and Experimental Therapeutics
Mol Pharmacol 76:766–777, 2009

Vol. 76, No. 4
57042/3514656
Printed in U.S.A.

Signal Transducer and Activator of Transcription 3 Is Required for Abnormal Proliferation and Survival of TSC2-Deficient Cells: Relevance to Pulmonary Lymphangioleiomyomatosis[S]

Elena A. Goncharova, Dmitry A. Goncharov, Gautam Damera, Omar Tliba, Yassine Amrani, Reynold A. Panettieri, Jr., and Vera P. Krymskaya

Pulmonary, Allergy, and Critical Care Division, Airways Biology Initiative, Department of Medicine (E.A.G., D.A.G., G.D., R.A.P., V.P.K), Abramson Cancer Center (V.P.K.), Cardiovascular Institute (V.P.K.), University of Pennsylvania, Philadelphia, Pennsylvania; Department of Pharmaceutical Sciences, School of Pharmacy, Thomas Jefferson University, Philadelphia, Pennsylvania (O.T.); and Department of Infection, Immunity, and Inflammation, University of Leicester School of Medicine, Leicester, United Kingdom (Y.A.)

Received April 21, 2009; accepted July 13, 2009

ABSTRACT

Tumor suppressor complex TSC1/TSC2 represents a key negative regulator of mammalian target of rapamycin (mTOR)-S6 kinase 1 signaling. Mutational inactivation of *TSC1* or *TSC2*, linked to a rare lung disease, lymphangioleiomyomatosis (LAM), manifests as neoplastic growth of smooth-muscle (SM)-like cells and cystic destruction of the lungs that induces loss of pulmonary function. However, the precise mechanisms of abnormal cell growth in LAM remain uncertain. Here, we demonstrate increased signal transducer and activator of transcription (STAT) 3 expression, phosphorylation, and nuclear localization in SM-like cells in LAM lungs and in TSC2-null xenographic tumors. Treatment of TSC2-null tumors with mTOR inhibitor rapamycin attenuated STAT3 expression and phosphorylation. Increased STAT3 level and activation were also observed in LAM-dissociated (LAMD) cell cultures compared with normal human bronchus fibroblasts (HBFs) from LAM patients. Although interferon (IFN)-γ inhibited proliferation of HBFs, IFN-γ treatment had little effect on proliferation of LAMD and TSC2-null cells. Re-expression of TSC2 or treatment with rapamycin inhibited IFN-γ-induced STAT3 phosphorylation and synergized with IFN-γ in inhibiting TSC2-null and LAMD cell proliferation. Reduction of STAT3 protein levels or activity using specific small interfering RNA or inhibitory peptide, respectively, decreased proliferation and induced apoptosis in TSC2-null and LAMD cells and sensitized cells to growth-inhibitory and proapoptotic effects of IFN-γ. Collectively, our data demonstrate that STAT3 activation is required for proliferation and survival of cells with TSC2 dysfunction, that STAT3 impedes growth-inhibitory and proapoptotic effects of IFN-γ, and that TSC2- and rapamycin-dependent inhibition of STAT3 restores antiproliferative effects of IFN-γ. Thus, STAT3 may provide a novel therapeutic target for diseases associated with TSC1/TSC2 dysfunction.

Tumor suppressors tuberous sclerosis complex (TSC) 1 and TSC2 belong to the phosphatidylinositol 3-kinase-mTOR signaling cascade, a key component of the highly conserved signal transduction network activated by growth-promoting signaling (Goncharova and Krymskaya, 2008). TSC1/TSC2 controls mTOR complex 1 (mTORC1)-S6 kinase 1 (S6K1) signaling by acting as a GTPase-activating protein toward small GTPase Rheb, a direct target of TSC2 GTPase-activating protein activity (Li et al., 2004). mTORC1 mediates three major inputs from growth factors, amino acids, and ATP and provides a master regulatory function for cell metabolism, proliferation, and apoptosis (Sabatini, 2006). In normal cells, mTORC1 signaling is tightly controlled. However, in pulmo-

This work was supported by the National Institutes of Health National Heart, Lung, and Blood Institute [Grants 2R01-HL071106, 1R01-HL090829, HL55301, HL64063, R00-HL089409-03]; the Abramson Cancer Center Pilot Project Grant; the American Thoracic Society/LAM Foundation [Grant LAM-07-001]; the American Lung Association [Grant RG-49342-N]; and the Parker B. Francis Fellowship.

Article, publication date, and citation information can be found at http://molpharm.aspetjournals.org.

doi:10.1124/mol.109.057042.

[S] The online version of this article (available at http://molpharm.aspetjournals.org) contains supplemental material.

ABBREVIATIONS: TSC, tuberous sclerosis complex; mTOR, mammalian target of rapamycin; RAPA, rapamycin; S6K1, S6 kinase 1; LAM, lymphangioleiomyomatosis; SM, smooth muscle; IFN, interferon; STAT, signal transducer and activator of transcription; JAK, Janus tyrosine kinase; MEF, mouse embryonic fibroblast; LAMD, lymphangioleiomyomatosis-dissociated; HBF, human bronchus fibroblast; PBS, phosphate-buffered saline; DAPI, 4,6-diamidino-2-phenylindole; siRNA, small interfering RNA; pEGFP, plasmid encoding for enhanced green fluorescent protein; PDGF, platelet-derived growth factor; BrdU, 5-bromo-2′-deoxyuridine; GFP, green fluorescent protein; ANOVA, analysis of variance; CCI-779, temsirolimus; NDRI, National Disease Research Interchange.

nary lymphangioleiomyomatosis (LAM), a rare lung disease, which could be sporadic or associated with TSC hamartoma syndrome, mutational inactivation of TSC1 or TSC2 induces the constitutive activation of mTORC1-S6K1 and neoplastic smooth muscle (SM)-like cell growth within the lung, leading to the cystic destruction of the lung and pneumothorax (for reviews, see Goncharova and Krymskaya, 2008; Krymskaya and Goncharova, 2009). Discovery of TSC1/TSC2 as a negative regulator of mTORC1 (Goncharova et al., 2002b) identified mTOR as a molecular target and mTOR inhibitor rapamycin (sirolimus; RAPA) as a therapeutic agent for treatment of LAM and TSC (Bissler et al., 2008; Krymskaya and Goncharova, 2009). However, the precise cellular and molecular mechanisms of LAM pathogenesis remain to be elucidated, and the need to identify novel molecular targets for potential combinational therapeutic approaches is urgent.

Interferons (IFNs) are pleiotropic cytokines and key components in the host surveillance against tumorigenesis as a result of their antiproliferative and proapoptotic properties (Platanias, 2005). The biological effects of IFNs, however, are highly cell type-, tissue-, and context-specific (Platanias, 2005). We demonstrated previously that type I IFN-β is expressed in LAM lungs, attenuates LAM and TSC2-null cell proliferation, and cooperates with TSC2 and rapamycin in its growth-inhibitory effects (Goncharova et al., 2008). Little is known about the function of type II IFN-γ in pulmonary LAM; however, studies indicate a potential modulatory role of IFN-γ in development of TSC tumors. Transgenic *Tsc2*(+/−) mice constitutively overexpressing IFN-γ in the liver have reduction in renal tumor development (Hino et al., 2002); and expression of the IFN-γ allele in TSC patients correlates with lower frequency of TSC-associated kidney angiomyolipomas (Dabora et al., 2002), suggesting that increased endogenous levels of IFN-γ may counteract to TSC1/TSC2-related tumor development. However, little is known about a role of IFN-γ in abnormal cell proliferation in LAM.

Binding of IFN-γ with its specific transmembrane receptors induces phosphorylation of signal transducer and activation of transcription (STAT) proteins, which dimerization and nuclear translocation promotes transcription of genes essential for regulation of cell proliferation, differentiation, development, and apoptosis (Platanias, 2005; Gough et al., 2008). Although IFN-γ inhibits proliferation and induces apoptosis through the canonical JAK-STAT1 signaling cascade (Platanias, 2005; Gough et al., 2008), it may also signal through the noncanonical STAT3 pathway, which is highly cell type- and context-specific (Gough et al., 2008). Constitutive activation of STAT3, frequently observed in different human tumors (Al Zaid Siddiquee and Turkson, 2008), prevents regression of xenographic hepatocellular carcinoma (Lin et al., 2009) and mouse melanoma tumors (Niu et al., 1999) and impedes growth-inhibitory and antiapoptotic effects of IFN-γ in cancer cell lines (Al Zaid Siddiquee and Turkson, 2008), suggesting that targeting STAT3 may have benefits in inhibiting tumor growth.

Few studies have investigated the role of TSC2-mTOR in IFN-γ signaling and in STAT3 activation. Indeed, mTOR activity is required for ^{Tyr705}STAT3 phosphorylation in monocytes, macrophages, and primary dendritic cells (Weichhart et al., 2008); and IFN-γ and rapamycin cooperate in suppressing ^{Tyr705}STAT3 phosphorylation in TSC2-null mouse embryonic fibroblasts (MEFs) (El-Hashemite et al., 2004). In contrast, mTOR is required for IFN-γ-dependent dephosphorylation of ^{Tyr705}STAT3 in human prostate cancer cells (Fang et al., 2006). mTOR also modulates IFN-γ-dependent transcriptional regulation through serine phosphorylation of STAT1, STAT3 (Nguyen et al., 2001; Riemenschneider et al., 2006; Zhou et al., 2007), and 4E-binding protein 1 (Kaur et al., 2007), but these effects seem to be JAK-STAT-independent (Kaur et al., 2007). Although these findings suggest the importance of mTOR in IFN-γ signaling, little is known about the relationship among TSC2-mTOR, IFN-γ, and STAT3 in pulmonary LAM.

The goal of our study was to determine the relationship among IFN-γ, STAT3, and TSC2-mTOR signaling in regulating cell proliferation. Our data demonstrate that STAT3 is necessary for abnormal proliferation and survival of cells with TSC2 dysfunction and that STAT3 activation prevents antiproliferative and proapoptotic activities of IFN-γ in LAM.

Materials and Methods

Tissue Preparation from LAM Lungs and TSC2-Null Tumors

Fresh LAM tissue samples were obtained from the National Heart, Lung, and Blood Institute (National Institutes of Health, Bethesda, MD) LAM Registry and the National Disease Research Interchange (NDRI; Philadelphia, PA). Normal human lung and normal trachea were obtained from tissue provided by National Disease Research Interchange. Tissue samples were snap-frozen in OCT embedding compound (Tissue-Tek, Tokyo, Japan), sectioned, and then subjected to immunohistochemical analysis. Xenographic TSC2-null tumors were obtained from athymic NCRNU-M female mice as follows: 5×10^6 TSC2-null rat SM α-actin-positive ELT3 cells, derived from Eker rat uterine leiomyoma (Howe et al., 1995), were injected subcutaneously into both flanks of 6-week-old NCRNU-M female mice; when tumors reached 5 mm in diameter, mice were subjected to treatment with rapamycin (intraperitoneal injections, three times a week; 4 mg/kg) or diluent (control). After 14 days, mice were euthanized; tumors were removed and snap-frozen in OCT embedding compound. Tumor tissue sections were subjected to immunohistochemical analysis as described below. Tissue samples from eight animals per each condition were examined.

Tissue Cell Culture

Experiments were performed using TSC2-null ELT3 cells (Howe et al., 1995) and LAMD cells, which were dissociated from LAM nodules of the lungs of LAM patients who have undergone lung transplant according to the protocol approved by the University of Pennsylvania Institutional Review Board. Fresh LAM tissue samples were provided by National Heart, Lung, and Blood Institute LAM Registry and NDRI. In brief, cells were dissociated by enzymatic digestion in M199 medium containing 0.2 mM $CaCl_2$, 2 mg/ml collagenase D (Hoffman-La Roche, Nutley, NJ), 1 mg/ml trypsin inhibitor (Sigma-Aldrich, St. Louis, MO), and 3 mg/ml elastase (Worthington Biochemicals, Lakewood, NJ). Then, the cell suspension was filtered and washed with equal volumes of ice-cold DF8 medium, consisting of equal amounts of Ham's F-12 and Dulbecco's modified Eagle's medium supplemented with 1.6×10^{-6} M ferrous sulfate, 1.2×10^{-5} units/ml vasopressin, 1.0×10^{-9} M triiodothyronine, 0.025 mg/ml insulin, 1.0×10^{-8} M cholesterol, 2.0×10^{-7} M hydrocortisone, 10 pg/ml transferrin, and 10% fetal bovine serum. The cells were cultured in DF8 medium and were passaged twice a week. LAMD cells from each patient were characterized on a basis of SM α-actin expression, S6K1 activity, ribosomal protein S6 phosphorylation, and DNA synthesis (Goncharova et al., 2002b, 2006a). All LAMD cells used in this study had constitutively activated S6K1,

hyperphosphorylated ribosomal protein S6, and a high degree of proliferative activity in the absence of any stimuli as well as a filamentous expression pattern of SM α-actin (Goncharova et al., 2002b, 2006a). LAMD cells in subculture during the third through 12th cell passages were used. Human bronchus fibroblasts (HBFs) were dissociated from the bronchus of the same LAM patients according to the protocol used for LAMD cell dissociation (Goncharova et al., 2002b, 2006a). Before experiments, cells were serum-deprived for 24 h. All experiments were performed on LAMD and HBF cell cultures from a minimum of three different LAM patients.

Immunohistochemical and Immunocytochemical Analysis

Tissue sections of LAM lung, normal human lung, normal human trachea, and TSC2-null tumors treated with diluent or rapamycin were immunostained with primary anti-phospho-^{Tyr705}STAT3, anti-total STAT3, anti-phospho-S6 (Cell Signaling Technology Inc., Danvers, MA), and anti-SM α-actin (Sigma-Aldrich) antibodies and then secondary Alexa Fluor 594 chicken anti-mouse or Alexa Fluor 488 chicken anti-rabbit IgG-conjugated antibodies (Invitrogen, Carlsbad, CA) (Goncharova et al., 2002b).

LAMD cells and HBFs, serum-deprived for 24 h, were fixed with 3.7% paraformaldehyde (Polysciences, Warrington, PA) for 15 min, incubated with 0.1% Triton X-100 (Sigma-Aldrich) for 30 min at room temperature, and then blocked with 2% bovine serum albumin in PBS followed by immunocytochemical analysis with anti-STAT3 antibody as described above. Negative controls included replacement of the primary antibody with isotype matched IgG. 4,6-Diamidino-2-phenylindole (DAPI) staining was performed to detect nuclei. Staining was visualized using an Eclipse E400 microscope (Nikon, Tokyo, Japan) under appropriate filters.

Transient Transfection

pEGFP and pEGFP-TSC2 expression vectors were prepared using EndoFree Plasmid Maxi kit (QIAGEN, Valencia, CA). siRNA GLO and siRNA STAT3 were purchased from Dharmacon RNA Technologies (Lafayette, CO). Transient transfection was performed using Effectene or RNAiFect transfection reagents (QIAGEN), respectively, according to the manufacturer's protocols. In brief, cells were incubated with pEGFP or pEGFP-TSC2 for 6 h and then washed with PBS and maintained in serum-free media for the next 24 h before DNA synthesis assays. For siRNA transfection, serum-deprived cells were incubated for 72 h with siRNA GLO or siRNA STAT3 followed by DNA synthesis assay or analysis of apoptosis. Expression of GFP-TSC2 was verified by immunoblot assay using anti-tuberin (C20) antibody (Santa Cruz Biotechnology, Inc., Santa Cruz, CA) (Goncharova et al., 2002b, 2008); depletion of STAT3 with siRNA STAT3 was verified by immunoblot analysis with anti-STAT3 antibodies as shown in Fig. 4A.

DNA Synthesis Analysis

[^{3}H]Thymidine Incorporation Assay. DNA synthesis was measured using [^{3}H]thymidine incorporation assay (Goncharova et al., 2006b). In brief, near-confluent human or rat cells, serum-deprived for 24 h, were incubated with different concentrations of human or rat IFN-γ, respectively, in the presence or absence of 200 nM rapamycin, 10 ng/ml PDGF, or both. After 18 h of incubation, cells were labeled with 3 μCi/ml [*methyl*-^{3}H]thymidine (60 Ci/mmol; GE Healthcare, Chalfont St. Giles, Buckinghamshire, UK) for 24 h. Then, cells were trypsinized and DNA was precipitated with 10% trichloroacetic acid. The precipitant was aspirated on glass filters and extensively washed, dried, and counted (Goncharova et al., 2006b).

BrdU Incorporation Assay. Nontransfected cells, or cells transfected with pEGFP-TSC2, pEGFP, siRNA STAT3, or siRNA GLO, were maintained for 24 h in serum-free medium, and then 5-bromo-2′-deoxyuridine (BrdU) incorporation was assessed (Goncharova et al., 2002b, 2006b). In brief, cells were treated with rapamycin, IFN-γ, or STAT3 inhibitory peptide (Calbiochem, Gibbstown, NJ), separately or in combination, or diluent in the presence or absence of 10 ng/ml PDGF for 18 h, and then 10 μM BrdU was added. After 24 h, cells were fixed with 3.7% paraformaldehyde (Polysciences) and then permeabilized with 0.1% Triton X-100 followed by immunocytochemical analysis with 2 μg/ml murine anti-BrdU primary (BD Biosciences, San Jose, CA) and 10 μg/ml Texas Red-conjugated anti-mouse secondary antibodies (Jackson ImmunoResearch Laboratories, West Grove, PA) to detect BrdU-positive cells. To identify GFP- and GFP-TSC2-transfected cells, immunocytochemical analysis with primary anti-GFP rabbit anti-serum, and then with Alexa Fluor 594 goat anti-rabbit IgG-conjugate (Invitrogen) was performed. To detect the total number of nuclei, cells were incubated with 1 μg/ml DAPI. Then, cells were examined using an Eclipse E400 microscope (Nikon) at 200× magnification with the appropriate fluorescent filters. The mitotic index of nontransfected or siRNA-transfected cells was defined as the percentage of BrdU-positive cells per field/total number of cells per field. The mitotic index of GFP- or GFP-TSC2-transfected cells was calculated as the percentage of BrdU-positive cells expressing GFP per total number of GFP-positive cells taken as 100%. In total, 200 cells were counted per each condition in each experiment.

Preparation of Cytoplasmic and Nuclear Extracts and Immunoblot Analysis

Cytoplasmic and nuclear extracts were prepared using NE-PER nuclear and cytoplasmic extraction reagents (Pierce Biotechnology, Rockford, IL) according to manufacturer's protocol. In brief, serum-deprived LAMD cells and HBFs were washed twice with PBS, trypsinized, and then subjected to nuclear-cytoplasmic fractionation using NE-PER reagents. Phospho-^{Tyr705}STAT3 and total STAT3 in nuclear and cytoplasmic fractions were then examined by SDS-polyacrylamide gel electrophoresis and immunoblot analysis with specific antibodies. Immunoblot analysis with anti-β-actin antibodies was performed to demonstrate equal gel loading.

Serum-deprived cells were transfected with pEGFP-TSC2, pEGFP, siRNA STAT3, or siRNA GLO or preincubated with 20 or 200 nM RAPA or diluent and then treated with 100 U/ml IFN-γ, 100 U/ml IFN-β, or vehicle for 30 min. Next, cells were lysed and whole cell lysates were subjected to SDS-polyacrylamide gel electrophoresis and immunoblot analysis with anti-phospho-^{Tyr705}STAT3, anti-total STAT3, anti-phospho-^{Tyr701}STAT1, anti-total STAT1, or anti-total actin antibodies (Cell Signaling Technology Inc.) (Goncharova et al., 2002b; Goncharova and Krymskaya, 2008).

Analysis of Apoptosis

Analysis of apoptosis was performed using an In Situ Cell Death Detection kit based on terminal deoxynucleotidyl transferase dUTP nick-end labeling technology (Hoffman-La Roche) according to the manufacturer's protocol. In brief, nontransfected cells or cells transfected with siRNA STAT3 or siRNA GLO were serum-deprived for 24 h and then incubated with 100 U/ml IFN-γ, 200 nM rapamycin, STAT3 inhibitory peptide, or diluent for 18 h. Then, cells were fixed with 3.7% paraformaldehyde for 15 min and treated with 0.1% Triton X-100 (Sigma-Aldrich) for 30 min at room temperature followed by 1-h incubation with terminal deoxynucleotidyl transferase dUTP nick-end labeling reaction mixture at 37°C. After incubation, cells were mounted in VECTASHIELD mounting medium (Vector Laboratories, Burlingame, CA) with DAPI to detect cell nuclei and then visualized on an Eclipse E400 microscope (Nikon) with appropriate filters. In total, 200 cells were counted per each condition in each experiment.

Data Analysis

Data points from individual assays represent the mean values ± S.E. Statistically significant differences among groups were assessed with the analysis of variance (ANOVA) (Bonferroni-Dunn), with

values of $p < 0.05$ sufficient to reject the null hypothesis for all analyses. All experiments were designed with matched control conditions within each experiment to enable statistical comparison as paired samples.

Results

IFN-γ Has Little Effect on LAMD and TSC2-Null ELT3 Cell Proliferation. Because the antiproliferative activity of IFN-γ is reported for some cell types (El-Hashemite et al., 2004; Platanias, 2005) and because evidence suggests that IFN-γ can attenuate development of TSC tumors (Dabora et al., 2002; Hino et al., 2002, 2003), we examined the effects of IFN-γ on proliferation of TSC2-null ELT3 cells and primary cells dissociated from the nodules from the lungs of LAM patients (LAMD cells) (Goncharova et al., 2002b, 2006a). ELT3 and LAMD cells were serum-deprived and treated with different concentrations of IFN-γ or diluent in the presence or absence of 10 ng/ml PDGF for 18 h, followed by DNA synthesis analysis. To investigate growth-inhibitory effects of IFN-γ on DNA synthesis in mesenchymal ELT3 and LAMD cells, we had chosen PDGF, a well established mitogen inducing DNA synthesis in mesenchymal cells, including airway and vascular smooth muscle cells (Goncharova et al., 2002a). Based on this evidence, we hypothesized that IFN-γ may modulate PDGF-induced TSC2-null and LAMD cell proliferation. It was surprising that we found that IFN-γ, used even at high concentrations of 100 and 1000 U/ml, had little effect on both basal and PDGF-induced proliferation of TSC2-null ELT3 cells (Fig. 1A). Likewise, IFN-γ in concentrations of 10 to 1000 U/ml also had little effect on DNA synthesis of both serum-deprived (Fig. 1B) and PDGF-stimulated LAMD cells (Fig. 1C). In contrast, 100 and 1000 U/ml IFN-γ significantly inhibited PDGF-induced proliferation of normal HBFs dissociated from the normal bronchus of LAM patients (Fig. 1C). These data demonstrate that although IFN-γ inhibits DNA synthesis of normal human fibroblasts, antiproliferative effect of IFN-γ is suppressed in LAMD and TSC2-null ELT3 cells.

To examine the possibility that lack of growth-inhibitory effects of IFN-γ may be due to changes in IFN-γ receptor levels, we performed flow cytometry analysis of LAMD cells, HBFs, and human airway smooth muscle cells with anti-IFN-γRα, and anti-IFN-γRβ antibodies. We found that both α and β subunits of IFN-γ receptor are expressed in LAMD cells at the levels comparable with human airway smooth muscle cells and HBFs (see Supplemental Fig. S1), suggesting that the lack of growth-inhibitory effects of IFN-γ on LAMD cell proliferation is not due to decrease in the receptor levels. In addition, IFN-γ-induced receptor-dependent phosphorylation of STAT1 at Tyr701 in both LAMD cells and in control HBFs were at comparable levels (see Supplemental Fig. S2). Together, these data indicate that decreased sensitivity of LAMD and TSC2-null ELT3 cells to the antiproliferative effects of IFN-γ is unlikely to be associated with changes in levels of IFN-γ receptor expression and activation or in alterations in STAT1 signaling.

STAT3 Is Activated in LAMD Cells. Because IFN-γ failed to inhibit LAMD cell proliferation and STAT3 is known to play a role in tumorigenesis, we examined STAT3 activation and expression levels in LAMD cells. Given that loss of TSC2 function leads to increased cell proliferation in the absence of any stimuli because of the constitutive activation of mTOR/S6K1 signaling (Goncharova et al., 2002b, 2006a), we performed experiments under serum-depleted conditions to eliminate activation of other growth-promoting signaling pathways. It is important that growth medium increases STAT3 phosphorylation levels in different cell types (Ni et al., 2003; Agarwal et al., 2007; Yoshiura et al., 2007). Because the focus of our study was to investigate a relationship between TSC2 loss and STAT3 activation in modulating cell proliferation, we performed experiments in the absence of serum to minimize the basal levels of STAT3 activation.

As seen in Fig. 2, STAT3 was localized in both cytoplasm

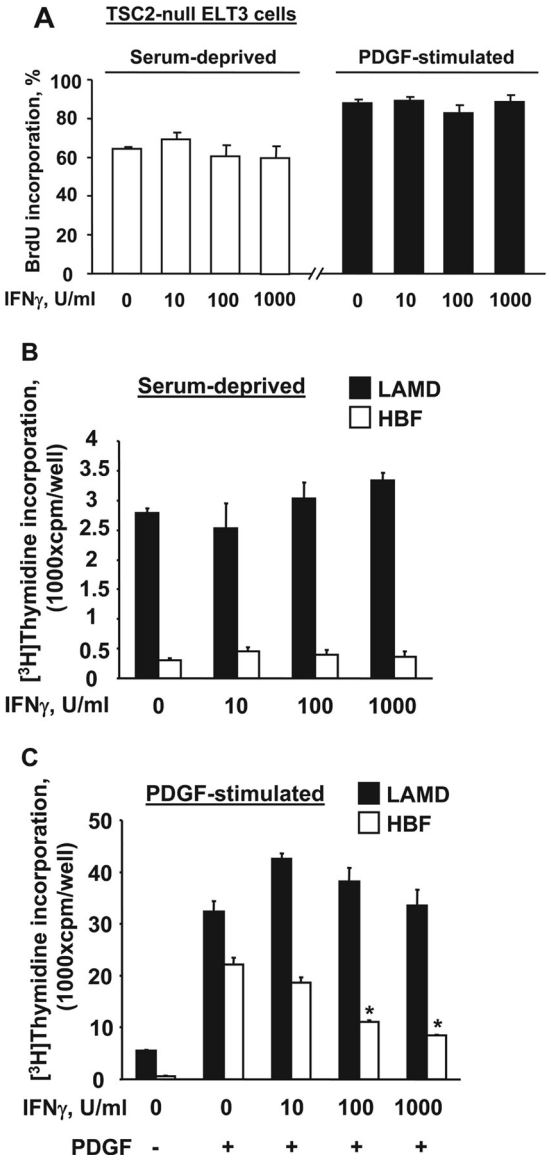

Fig. 1. IFN-γ has little effect on LAMD and TSC2-null ELT3 cell proliferation. A, serum-deprived ELT3 cells were treated with 10, 100, and 1000 U/ml rat IFN-γ or diluent for 18 h in the absence or presence 10 ng/ml PDGF followed by BrdU incorporation assay. Data represent mean values ± S.E. from three independent experiments by ANOVA (Bonferroni-Dunn). B and C, serum-deprived LAMD cells and HBFs were treated with 10, 100, and 1000 U/ml human IFN-γ or diluent for 18 h in the absence (B) or presence (C) of 10 ng/ml PDGF followed by [^{3}H]thymidine incorporation assay. Data represent mean values ± S.E. from three independent experiments. *, $p < 0.001$ for HBFs treated with 100 U/ml IFN-γ + PDGF or 1000 U/ml IFN-γ + PDGF versus PDGF-treated HBFs by ANOVA (Bonferroni-Dunn).

and nuclei of serum-depleted LAMD cells in contrast to predominantly cytoplasmic STAT3 localization in normal HBFs. Statistical analysis demonstrates that 67.3 ± 1.7% of serum-deprived LAMD cells had STAT3 nuclear localization compared with 22.9 ± 1.7% for HBFs (Fig. 2B). Analysis of STAT3 phosphorylation levels in cytoplasmic and nuclear compartments also shows that STAT3 was phosphorylated in nuclear fraction of serum-deprived LAMD cells but not in normal HBFs (Fig. 2C). In addition, total STAT3 levels were increased in LAMD cells compared with HBFs (Fig. 2C). Taken together, these data show that STAT3 is activated in LAMD cells in the absence of any stimuli.

Increased STAT3 Expression and Phosphorylation in SM-Like Cells in LAM Lungs and in TSC2-Null Tumors. To determine the relevance of our in vitro findings to pulmonary LAM, we analyzed STAT3 status in tissue sections from the lungs of four LAM patients using dual immunohistochemical analysis. Our previous studies demonstrate that loss of TSC2 function leads to the constitutive activation of mTOR/S6K1 signaling pathway in SM α-actin-positive cells forming LAM nodules (Goncharova et al., 2002b). Thus, we examined STAT3 expression and phosphorylation levels

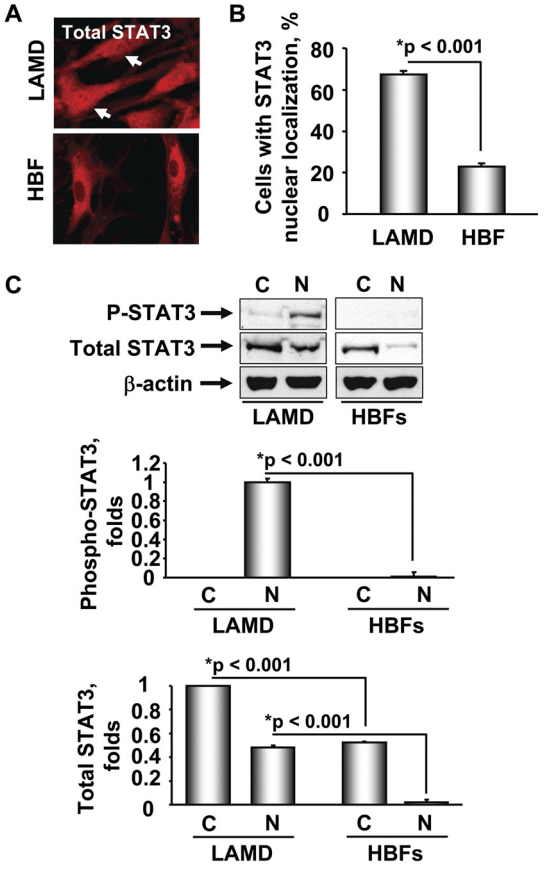

Fig. 2. STAT3 is activated in nonstimulated LAMD cells. A, immunocytochemical analysis of serum-deprived LAMD cells and HBFs with anti-STAT3 antibody. Representative images of three separate experiments were taken using a TE2000E microscope (Nikon) at 400× magnification. B, statistical analysis of three independent experiments. Data represent a percentage of cells with STAT3 nuclear localization per total number of cells. Data are mean values ± S.E. by ANOVA (Bonferroni-Dunn). At minimum, 60 cells per each condition were analyzed in each experiment. C, cytoplasmic (C) and nuclear (N) fractions of serum-deprived LAMD cells and HBFs were subjected to immunoblot analysis with anti-phospho-^{Tyr705}STAT3, anti-total STAT3, and anti-β-actin antibodies. Top, representative images of two independent experiments. Middle and bottom, statistical analysis of two independent experiments. Phospho-STAT3 optical density (OD) in nuclear fraction of LAMD cells (middle) or total STAT3 OD in cytoplasmic fraction of LAMD cells (bottom) was taken as one-fold.

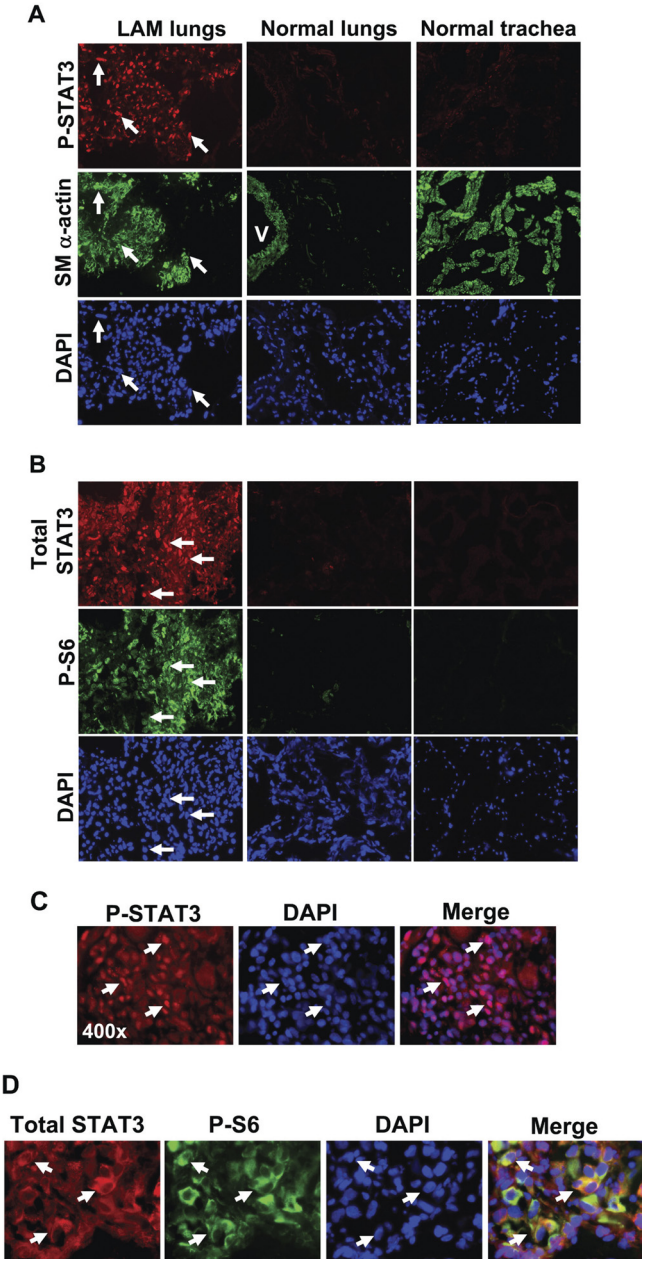

Fig. 3. Increased STAT3 expression and phosphorylation in SM-like cells in LAM lungs (A and B) and in TSC2-null tumors (C and D). Tissue specimens from the lungs of LAM patients (LAM lungs), normal human lungs, and normal human trachea were subjected to dual immunohistochemical analysis with anti-phospho-^{Tyr705}STAT3 (red) and anti-SM α-actin (green) (A); or anti-total STAT3 (red) and anti-phospho-S6 (green) antibodies (B). DAPI staining (blue) was performed to visualize the nuclei. Representative images from four LAM patients were taken using an Eclipse E400 microscope (Nikon) at 400× magnification. Arrows indicate phospho-STAT3 (A) or total STAT3 (B) nuclear localization. V, blood vessel. C and D, TSC2-null xenographic tumors in NCRNU-M nude female mice were subjected to immunohistochemical analysis with anti-phospho-^{Tyr705}STAT3 (red) antibody (C) or dual immunostaining with anti-total STAT3 (red) and anti-phospho-S6 (green) antibodies (D). Arrows indicate cells with nuclear localization of phospho-STAT3 (C) or cells with colocalization of cytosolic total STAT3 and phospho-S6 (D). Images are representative of two independent experiments. Images were taken using an Eclipse E400 microscope at 400× magnification with appropriate filters.

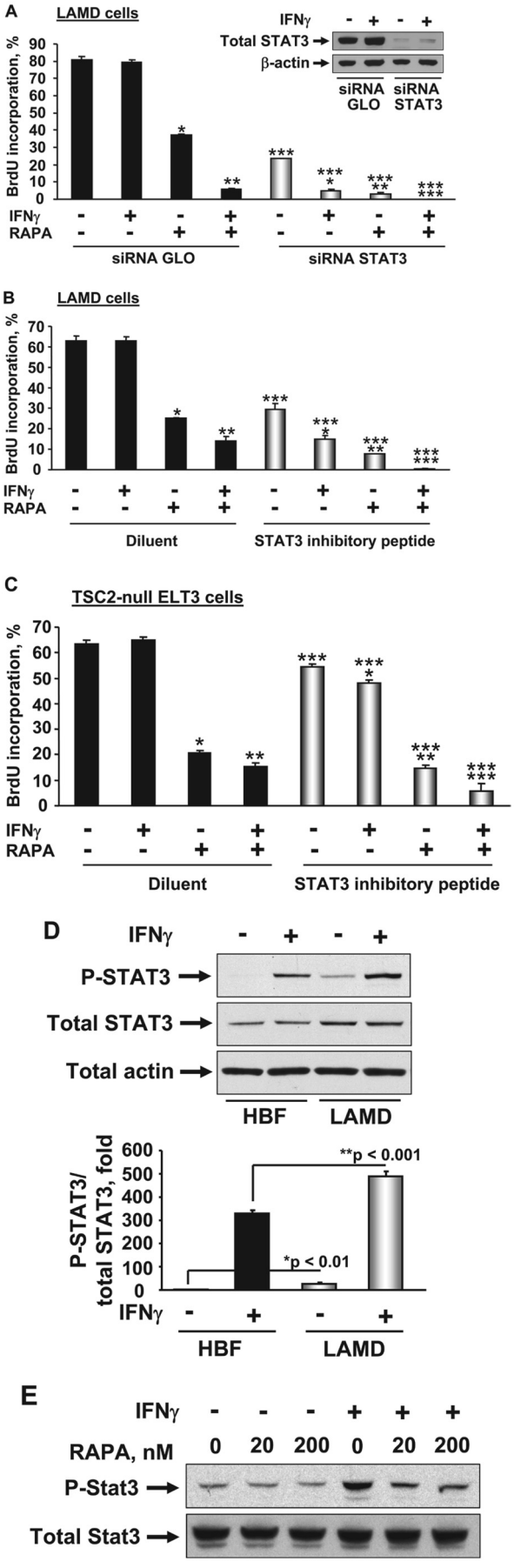

in SM α-actin-positive cells with hyperphosphorylated ribosomal protein S6, which is a molecular signature of activated mTOR/S6K1 signaling pathway (Goncharova et al., 2002b). Normal human lungs and normal human trachea were used as controls. As seen in Fig. 3A, STAT3 phosphorylation was detected in the nuclei of SM α-actin-positive cells in LAM lungs. In contrast, SM cells from blood vessels in normal lung and SM cells in trachea did not stain positively for phospho-STAT3 (Fig. 3A). Double immunostaining with anti-total STAT3 and anti-phospho-S6 antibodies demonstrated that phospho-S6-positive cells in LAM lungs also stained positively for STAT3 (Fig. 3B); however, modest STAT3 levels were detected in normal human lungs and trachea (Fig. 3B). It is important that total STAT3 protein, in addition to cytoplasmic localization, was also found in the nuclei of cells that had increased ribosomal protein S6 phosphorylation in LAM lungs (Fig. 3B), which correlates with translocation of activated STAT3 to the nuclei (Platanias, 2005). Taken together, these data show that STAT3 expression and nuclear phosphorylation are increased in SM α-actin- and phospho-S6-positive cells forming LAM nodules in the lungs of LAM patients.

Fig. 4. A to C, STAT3 is required for abnormal proliferation of LAMD and ELT3 cells. A, LAMD cells were transfected with siRNA STAT3 or control siRNA GLO for 72 h, serum-deprived for 24 h, and then treated with 100 U/ml IFN-γ, 200 nM RAPA, separately or in combination, or diluent for 18 h followed by BrdU incorporation assay. Data represent a percentage of BrdU-positive cells per total number of cells. Data represent means + S.E. from three independent experiments. *, $p < 0.001$ for siRNA GLO + RAPA versus siRNA GLO; **, $p < 0.001$ for siRNA GLO + RAPA + IFN-γ versus siRNA GLO + RAPA; ***, $p < 0.001$ for siRNA STAT3 versus siRNA GLO; ****, $p < 0.001$ for siRNA STAT3 + IFN-γ versus siRNA STAT3; *****, $p < 0.001$ for siRNA STAT3 + RAPA versus siRNA STAT3; ******, $p < 0.01$ for siRNA STAT3 + IFN-γ + RAPA versus siRNA STAT3 + IFN-γ or siRNA STAT3 + RAPA by ANOVA (Bonferroni-Dunn). STAT3 knockdown by siRNA STAT3 was confirmed by immunoblot analysis with anti-STAT3 and anti-β-actin antibodies to detect equal loading (top). B and C, serum-deprived for 24 h LAMD (B) and ELT3 (C) cells were treated with 100 μM STAT3 inhibitory peptide, 100 U/ml IFN-γ, 200 nM RAPA, or diluent, separately or in the combination, for 18 h, and then BrdU incorporation assay was performed. Data represent a percentage of BrdU-positive cells per total number of cells. Data represent means + S.E. from three independent experiments. B, *, $p < 0.001$ for RAPA versus diluent; **, $p < 0.01$ for RAPA + IFN-γ versus RAPA; ***, $p < 0.001$ for STAT3 inhibitory peptide versus diluent; ****, $p < 0.001$ for STAT3 inhibitory peptide + IFN-γ versus STAT3 inhibitory peptide; *****, $p < 0.001$ for STAT3 inhibitory peptide + RAPA versus STAT3 inhibitory peptide; ******, $p < 0.001$ for STAT3 inhibitory peptide + IFN-γ + RAPA versus STAT3 inhibitory peptide + IFN-γ or STAT3 inhibitory peptide + RAPA. C, *, $p < 0.001$ for RAPA versus diluent; **, $p < 0.05$ for RAPA + IFN-γ versus RAPA; ***, $p < 0.01$ for STAT3 inhibitory peptide versus diluent; ****, $p < 0.02$ for STAT3 inhibitory peptide + IFN-γ versus STAT3 inhibitory peptide; *****, $p < 0.001$ for STAT3 inhibitory peptide + RAPA versus STAT3 inhibitory peptide; ******, $p < 0.001$ for STAT3 inhibitory peptide + IFN-γ + RAPA versus STAT3 inhibitory peptide + IFN-γ or STAT3 inhibitory peptide + RAPA by ANOVA (Bonferroni-Dunn). D, effect of IFN-γ on STAT3 phosphorylation. Serum-deprived LAMD cells and HBFs were treated with 100 U/ml IFN-γ or diluent for 30 min followed by immunoblot analysis with anti-phospho-^{Tyr705}STAT3, anti-total STAT3, and anti-total actin antibodies. Top, representative images of three independent experiments. Bottom, statistical analysis of experiments. Phospho-STAT3 optical density (OD) per total STAT3 OD in diluent-treated LAMD cells was taken as one-fold. Data represent means + S.E. from three independent experiments by ANOVA (Bonferroni-Dunn). E, rapamycin inhibits IFN-γ-dependent STAT3 phosphorylation in TSC2-null ELT3 cells. Serum-deprived cells were preincubated with 20 and 200 nM RAPA, or diluent for 18 h, and then treated with 100 U/ml IFN-γ or vehicle for 30 min, and cell lysates were then subjected to immunoblot analysis with anti-phospho-^{Tyr705}STAT3 or anti-STAT3 antibodies. Images are representative of two separate experiments.

Given that pulmonary LAM is associated with TSC2 dysfunction (Goncharova et al., 2002b; Goncharova and Krymskaya, 2008), we next determined STAT3 activation status in xenographic TSC2-null tumors in athymic NCRNU-M female mice. Immunohistochemical analysis of TSC2-null tumors showed marked levels of STAT3 in cells with increased S6 phosphorylation (Fig. 3D). Apparent lack of STAT3 in the nucleus may reflect a limitation of immunohistochemical analysis with total STAT3 antibody; therefore, we used immunostaining with phospho-STAT3. As seen in Fig. 3C, activated STAT3 predominantly localizes in the nucleus in the tissue section from the same tumor tissue. Collectively, these data demonstrate that STAT3 is activated in SM α-actin-positive cells in LAM lungs and in TSC2-null tumors and show a correlation between our in vitro and in vivo findings.

STAT3 Is Required for Increased Proliferation and Survival of LAMD and TSC2-Null ELT3 Cells. To examine whether STAT3 is required for increased proliferation and survival of LAMD and TSC2-null ELT3 cells, we used two different approaches: down-regulation of endogenous STAT3 protein levels with specific siRNA STAT3 (Fig. 4A, top) and inhibition of STAT3 activity with STAT3 inhibitory peptide, which selectively blocks constitutive and ligand-induced STAT3 activation by disruption of STAT3:STAT3 dimerization and STAT3-DNA binding (Turkson et al., 2001). As seen in Fig. 4A, knockdown of endogenous STAT3 protein levels with siRNA markedly inhibited proliferation of serum-deprived LAMD cells compared with cells transfected with control siRNA GLO. The STAT3 inhibition with inhibitory peptide significantly decreased DNA synthesis in LAMD cells compared with the diluent-treated cells (Fig. 4B). It is interesting that STAT3 inhibitory peptide only attenuated the proliferation of rat TSC2-null cells (Fig. 4C), suggesting that a lesser inhibitory effect may occur as a result of the differential effect of STAT3 inactivation depending on species and cell type.

To determine a requirement of STAT3 for LAMD cell survival, we next examined apoptosis in LAMD cells transfected with siRNA STAT3 or treated with STAT3 inhibitory peptide (Fig. 5). Our data demonstrate that either depletion of STAT3 endogenous protein levels or inhibition of STAT3 activity induced apoptosis compared with cells transfected with siRNA GLO or treated with diluent (Fig. 5, A and B, respectively). Collectively, these data demonstrate that STAT3 is required for increased proliferation and survival of cells with TSC2 dysfunction.

Next, we examined whether STAT3 down-regulation with siRNA and STAT3 inactivation with inhibitory peptide modulate effects of IFN-γ on cell proliferation and apoptosis. As shown in Fig. 4A, IFN-γ had little effect on the proliferation of cells transfected with control siRNA GLO (Fig. 4A, black bars); in contrast, when STAT3 levels were down-regulated with siRNA, IFN-γ significantly inhibited LAMD cell proliferation (Fig. 4A, gray bars). Similar results were obtained using STAT3 inhibitory peptide: IFN-γ had little effect on proliferation of diluent-treated LAMD and TSC2-null ELT3 cells (Fig. 4, B and C, black bars) but augmented STAT3 inhibitory peptide in inhibiting cell growth (Fig. 4, B and C, gray bars). We also examined whether STAT3 modulates antiapoptotic functions of IFN-γ. IFN-γ had little effect on the levels of apoptotic cells transfected with control siRNA GLO or treated with diluent (Fig. 5, A and B, black bars). It is important that IFN-γ further enhanced apoptosis induced by down-regulation of STAT3 protein levels or inhibition of STAT3 activity (Fig. 5, A and B, gray bars), demonstrating that STAT3 also impedes proapoptotic effects of IFN-γ in LAMD cells.

To examine the relationship between STAT3 and IFN-γ signaling, we examined whether IFN-γ affects STAT3 phosphorylation. As seen in Fig. 4, D and E, IFN-γ enhanced STAT3 phosphorylation in LAMD and TSC2-null ELT3 cells; IFN-γ also activated STAT3 in normal HBFs. Quantitative analyses demonstrate that phospho-STAT3/total STAT3 ratio was even higher in IFN-γ-treated LAMD cells versus IFN-γ-treated HBFs (Fig. 4D, bottom). Given that IFN-γ has similar effects on STAT3 activation in LAMD and HBFs and has opposite effects on cell proliferation, we speculate that IFN-γ-dependent STAT3 signaling is either dysregulated downstream of STAT3 or that STAT3 signaling does not converge with growth-inhibitory and proapoptotic signaling pathways activated by IFN-γ in LAMD cells.

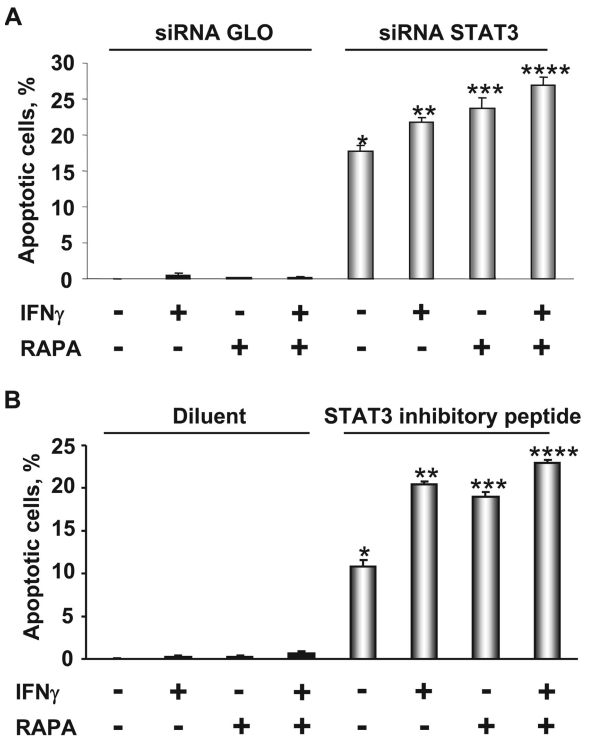

Fig. 5. STAT3 is required for LAMD cell survival. A, serum-deprived cells, transfected with siRNA STAT3 or control siRNA GLO for 72 h, were treated with 100 U/ml IFN-γ, 200 nM RAPA or diluent, separately or in combination, for 24 h followed by apoptosis analysis with In Situ Cell Death Detection kit. Data represent percentage of apoptotic cells per total number of cells. At minimum, 60 cells were analyzed in each experiment per each condition. Data represent mean values + S.E. from two independent experiments. *, $p < 0.001$ for siRNA STAT3 versus siRNA GLO; **, $p < 0.01$ for siRNA STAT3 + IFN-γ versus siRNA STAT3; ***, $p < 0.001$ for siRNA STAT3 + RAPA versus siRNA STAT3; ****, $p < 0.05$ for siRNA STAT3 + IFN-γ + RAPA versus siRNA STAT3 + IFN-γ or siRNA STAT3 + RAPA. B, serum-deprived cells were treated with 100 μM STAT3 inhibitory peptide, 100 U/ml IFN-γ, 200 nM RAPA, or diluent, separately or in combination, for 24 h, and then apoptosis analysis with In Situ Cell Death Detection kit was performed. *, $p < 0.001$ for STAT3 inhibitory peptide versus diluent; **, $p < 0.001$ for STAT3 inhibitory peptide + IFN-γ versus STAT3 inhibitory peptide; ***, $p < 0.001$ for STAT3 inhibitory peptide + RAPA versus STAT3 inhibitory peptide; ****, $p < 0.01$ for STAT3 inhibitory peptide + IFN-γ + RAPA versus STAT3 inhibitory peptide + IFN-γ or STAT3 inhibitory peptide + RAPA by ANOVA (Bonferroni-Dunn).

Rapamycin and IFN-γ Synergistically Inhibit TSC2-Null ELT3 and LAMD Cell Proliferation. Because LAM is associated with loss of TSC2 function, which promotes activation of mTOR/S6K1 (Goncharova et al., 2002b, 2006a, 2008), we examined whether TSC2 and/or mTOR are involved in modulation of STAT3 and IFN-γ-dependent signaling in LAMD and TSC2-null ELT3 cells (Figs. 4 and 6). Cells were treated with different concentrations of IFN-γ and 200 nM rapamycin, separately or in combination, in the presence or absence of PDGF for 18 h followed by DNA synthesis analysis. We chose a concentration of rapamycin at 200 nM because this concentration abrogates the constitutive activation of S6K1 and maximally inhibits LAMD and TSC2-null ELT3 cell proliferation, as we demonstrated in our previous studies (Goncharova et al., 2002b, 2006a, 2008). As shown in Fig. 6A and as we demonstrated previously (Goncharova et al., 2008), rapamycin inhibited TSC2-null ELT3 cell proliferation in serum-deprived conditions. IFN-γ alone had little effect on TSC2-null ELT3 cell proliferation, but the combination of IFN-γ and rapamycin further inhibited both basal and PDGF-induced cell proliferation compared with either agent alone (Fig. 6A). Similar results were obtained for LAMD cells, which were treated with different concentrations of IFN-γ in the presence or absence of rapamycin. Rapamycin markedly reduced both basal and PDGF-induced proliferation of LAMD cells (Fig. 6, B and C). It is important that although IFN-γ alone had little effect on LAMD cell proliferation (Fig. 6, B and C, black bars), the combination of IFN-γ and rapamycin markedly inhibited basal and PDGF-induced cell proliferation compared with effects of IFN-γ and rapamycin given separately, and this effect was dependent of IFN-γ concentration (Fig. 6, B and C, respectively, gray bars).

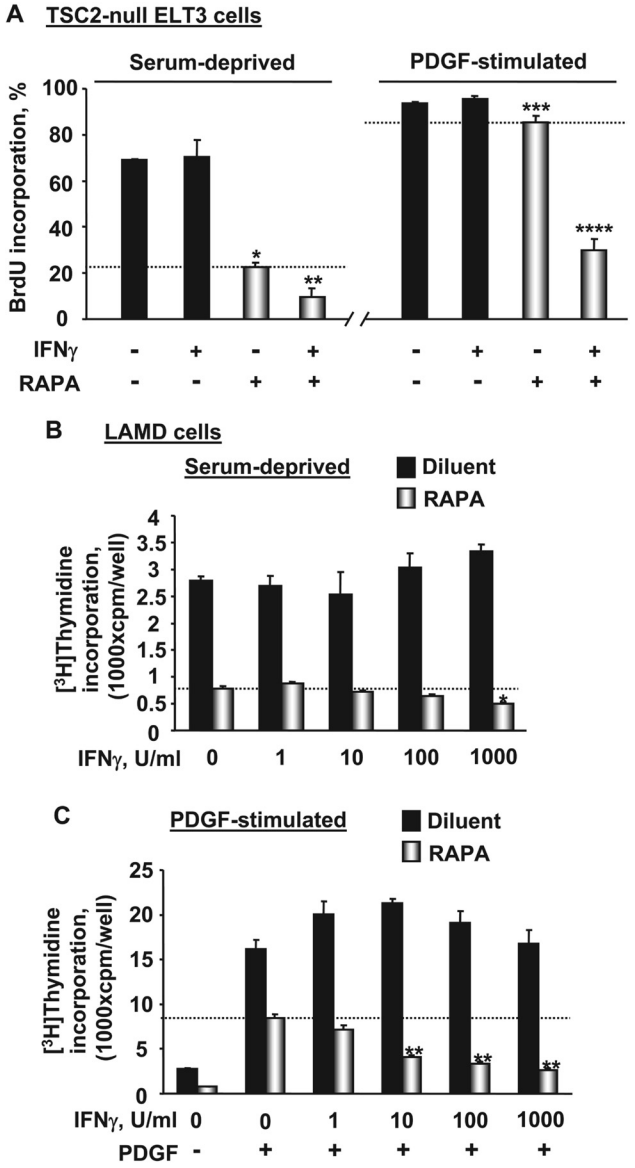

Fig. 6. Rapamycin and IFN-γ have synergistic inhibitory effects on TSC2-null ELT3 and LAMD cell proliferation. A, serum-deprived ELT3 cells were preincubated with 200 nM RAPA, 100 U/ml rat IFN-γ, 200 nM RAPA + 100 U/ml IFN-γ, or diluent in the presence or absence of 10 ng/ml PDGF for 18 h followed by BrdU incorporation analysis. Data represent mean values + S.E. from three independent experiments. *, $p < 0.001$ for RAPA versus control and IFN-γ; **, $p < 0.01$ for IFN-γ + RAPA versus IFN-γ and RAPA; ***, $p < 0.05$ for RAPA + PDGF versus PDGF; ****, $p < 0.001$ for IFN-γ + RAPA + PDGF versus IFN-γ + PDGF and RAPA + PDGF. B and C, LAMD cells, serum-deprived (B) or treated with 10 ng/ml PDGF (C), were incubated with 1, 10, 100, and 1000 U/ml human IFN-γ or diluent in the presence or absence of 200 nM RAPA for 18 h, and then the [^{3}H]thymidine incorporation assay was performed. Data represent mean values + S.E. from three independent experiments. Dotted lines indicate the levels of DNA synthesis in rapamycin-treated cells. *, $p < 0.01$ for 1000 U/ml IFN-γ + RAPA versus RAPA and IFN-γ; **, $p < 0.001$ for PDGF + IFN-γ + RAPA versus PDGF + RAPA and PDGF + IFN-γ by ANOVA (Bonferroni-Dunn).

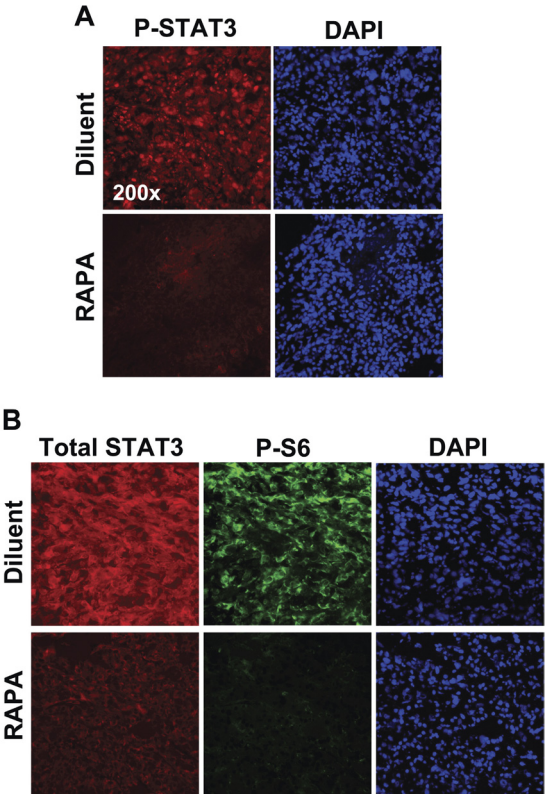

Fig. 7. Rapamycin abrogates STAT3 phosphorylation and attenuates total STAT3 protein levels in TSC2-null tumors. TSC2-null ELT3 cells (5×10^6) were injected in flanks of NCRNU-M female mice. When tumors reached 5 mm in diameter, mice were treated with diluent or rapamycin for 14 days. Then mice were sacrificed, and immunohistochemical analysis of tumors was performed with anti-phospho-^{Tyr705}STAT3 antibody (red; A), or tumors were subjected to dual immunohistochemical analysis with anti-total STAT3 (red) and anti-phospho-S6 (green) antibodies (B). DAPI staining (blue) was performed to detect the nuclei. Images are representative of eight animals per each condition. Images were taken at 200× magnification using an Eclipse E400 microscope (Nikon).

Although rapamycin significantly inhibited cell proliferation and combined with IFN-γ to abrogate DNA synthesis (Figs. 4, black bars; and 6), it had little effect on the levels of apoptotic cells and did not synergize with IFN-γ to induce apoptosis (Fig. 5, black bars). These data suggest that rapamycin- and IFN-γ-dependent inhibition of cell growth may not be due to induction of apoptosis.

Inhibition of mTOR activity by rapamycin decreased IFN-γ-induced STAT3 phosphorylation (Fig. 4E); however, rapamycin had little effect on basal STAT3 phosphorylation (Fig. 4E), suggesting that mTOR modulates IFN-γ-dependent STAT3 phosphorylation. To examine the relationship between mTOR and STAT3 in modulating cell proliferation and apoptosis in cells with TSC2 dysfunction, DNA synthesis was examined in serum-deprived cells, transfected with siRNA STAT3 or treated with STAT3 inhibitory peptide, incubated with 200 nM rapamycin, 100 U/ml IFN-γ, or diluent, separately or in combination. Rapamycin alone, as we described previously, markedly inhibited DNA synthesis and synergized with IFN-γ in inhibition of proliferation of siRNA GLO-transfected or diluent-treated LAMD cells (Fig. 4, black bars). Rapamycin further reduced proliferation of cells transfected with siRNA STAT3 or treated with STAT3 inhibitory peptide (Fig. 4, gray bars), suggesting that mTOR and STAT3 act in parallel to maintain increased proliferation of nonstimulated LAMD and TSC2-null ELT3 cells. In addition, rapamycin cooperated with IFN-γ in inhibition of DNA synthesis in cells with depleted STAT3 protein or inhibited STAT3 activity (Fig. 4, gray bars), suggesting that rapamycin, in addition to restoring antiproliferative effects of IFN-γ, modulates cell proliferation via alternative mechanism.

Analysis of apoptosis, performed under the same experimental conditions, demonstrated that neither rapamycin nor IFN-γ, separately or in combination, promoted apoptosis in siRNA GLO-transfected or diluent-treated LAMD cells (Fig. 5, A and B, respectively, black bars). In cells with suppressed STAT3 endogenous protein levels or activity, IFN-γ or rapamycin alone augmented apoptosis caused by siRNA STAT3 or STAT3 inhibitory peptide; however, when given simultaneously, they did not additively promote apoptosis (Fig. 5, A and B, respectively, gray bars). These data suggest that rapamycin has little effect on proapoptotic function of IFN-γ.

We also examined whether rapamycin affects STAT3 in vivo. Athymic NCRNU-M female mice with subcutaneous rat TSC2-null tumors were treated with specific mTOR inhibitor rapamycin or diluent for 14 days. We found that treatment with rapamycin led to suppression of ribosomal protein S6 phosphorylation (Fig. 7B, bottom). Rapamycin also abrogated STAT3 phosphorylation and attenuated total STAT3 protein levels in TSC2-null tumors compared with tumors treated with diluent (Fig. 7, A and B, respectively). These data demonstrate that rapamycin inhibits STAT3 activation and attenuates STAT3 levels in vivo.

Re-expression of TSC2 Restores Inhibitory Effect of IFN-γ on Cell Proliferation. Because abnormal cell proliferation in LAM is associated with TSC2 dysfunction, we next examined whether re-expression of TSC2 will restore the antiproliferative activity of IFN-γ. TSC2-null ELT3 and LAMD cells were transfected with plasmids expressing GFP-TSC2 or control GFP, treated with 100 U/ml IFN-γ or diluent in the presence or absence of 10 ng/ml PDGF for 18 h, and then DNA synthesis was measured using BrdU incorporation assay. As shown in Fig. 8A, re-expression of TSC2 inhibited TSC2-null ELT3 cell proliferation, as we demonstrated previously (Goncharova et al., 2002b, 2008). IFN-γ had little effect on both basal and PDGF-induced proliferation of control transfected cells (Fig. 8A, black bars). In contrast, treatment of TSC2-transfected cells with IFN-γ augmented TSC2-dependent inhibition of cell proliferation (Fig. 8A, gray bars), suggesting that TSC2 is required for growth inhibitory effects of IFN-γ. Likewise, IFN-γ had little effect on proliferation of GFP-transfected LAMD cells (Fig. 8B, black bars) but significantly augmented inhibitory effect of TSC2 on cell proliferation (Fig. 8B, gray bars). In parallel, we examined the effect of TSC2 on STAT3 phosphorylation. As seen in Fig. 8, C and D, black bars, GFP-transfected TSC2-null ELT3 and LAMD cells had modest basal STAT3 phosphorylation, which was further increased by IFN-γ. Re-expression of TSC2 had little effect on basal phosphorylation of STAT3 and on STAT3 protein levels, but markedly inhibited IFN-γ-dependent STAT3 phosphorylation compared with GFP-transfected cells (Fig. 8, C and D, gray bars). Although our in vivo data (Fig. 7) show strong correlation between loss of TSC2 function and STAT3 phosphorylation, re-expression of TSC2, however, only partially inhibited STAT3 phosphorylation in TSC2-null ELT3 and LAMD cells. These differences may be explained by experimental limitations associated with transient transfection technique. Transfection efficiency for TSC2 vector was approximately 25 to 35% of total cell population. Because immunoblot analysis technique does not allow to separate transfected and nontransfected cells, it is highly possible that re-expression of TSC2 was not sufficient to markedly inhibit phospho-STAT3 detected by immunoblot analysis. Given that TSC2 regulates activity of mTORC1/S6K1 and protein synthesis, another possible explanation is that TSC2 modulates STAT3 phosphorylation through modulation of synthesis of the proteins involved in regulating phospho-STAT3 levels. Because TSC2 re-expression time during transient transfection is limited to 24 h to avoid toxic effects of TSC2 overexpression, this period of time may not be sufficient to fully reconstitute long-term effects on protein synthesis. Collectively, these data demonstrate that TSC2 expression modulates IFN-γ-induced STAT3 phosphorylation and restores the antiproliferative activity of IFN-γ in both TSC2-null ELT3 and LAMD cells.

Discussion

Understanding the cellular and molecular mechanisms of neoplastic cell proliferation in pulmonary LAM is critically important for identifying novel therapeutic approaches to treat LAM. Here, we show that loss of TSC2 function in LAM is associated with activation of STAT3, which is required for cell proliferation and impedes growth-inhibitory and proapoptotic functions of IFN-γ.

IFN-γ has proven antiproliferative and proapoptotic activities (Platanias, 2005) and may counteract tumor development in TSC. Correlation between high-expressing IFN-γ allele and reduced frequency of kidney angiomyolipoma was reported in patients with TSC (Dabora et al., 2002), and endogenous expression of high levels of IFN-γ is associated with reduction in kidney tumor development in *Tsc2*(+/−) mice (Hino et al., 2002). However, preclinical studies testing IFN-γ as a potential therapeutic agent for TSC remain in-

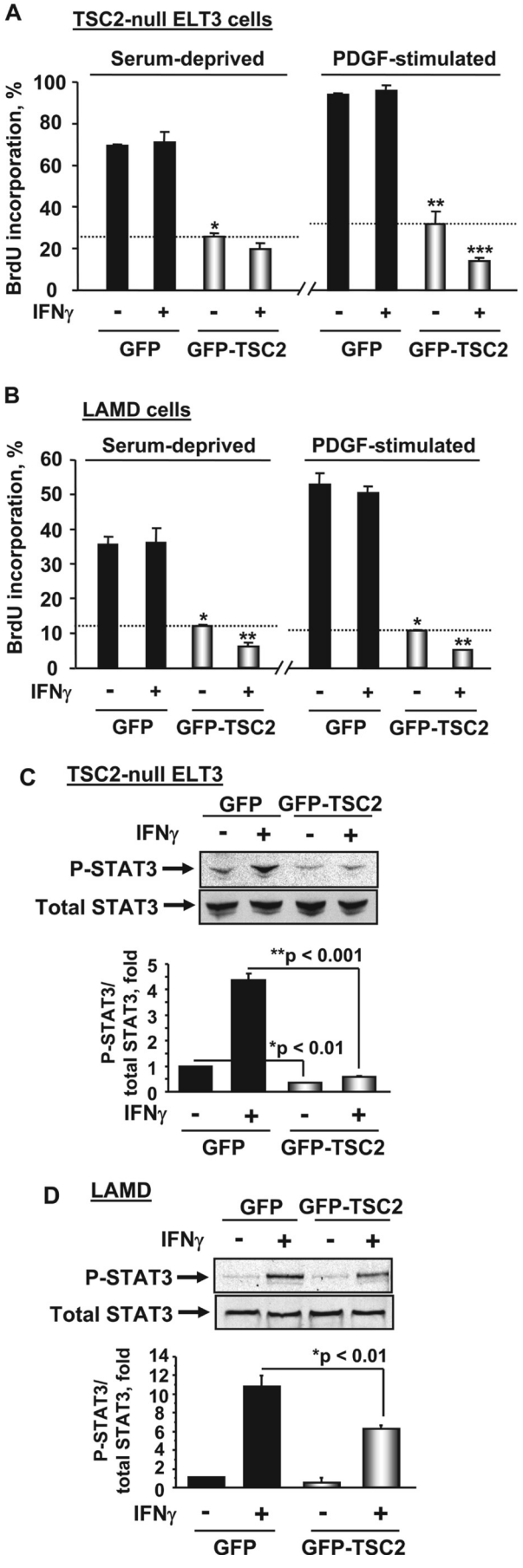

conclusive. Although treatment with IFN-γ either as a single agent or in combination with rapamycin analog CCI-779 improves survival of *Tsc2*(+/−) mice (Lee et al., 2005) and decreases subcutaneous TSC2-null tumor growth at the early stages of tumor development (Lee et al., 2006), the simultaneous treatment of *Tsc2*(+/−) mice from 6 to 8 or 10 to 12 months of age with IFN-γ does not enhance antitumor activity of CCI-779; furthermore, IFN-γ treatment from 2 to 4 months of age reverses CCI-779 tumor-suppressing function (Messina et al., 2007). These differences may occur because of differential effects of IFN-γ on tumor growth during various stages of tumor development (Platanias, 2005). Thus, although IFN-γ may inhibit new tumor growth, already established tumors may be refractory to IFN-γ treatment. Further studies are needed to evaluate effects of IFN-γ on TSC1/TSC2-related tumorigenesis. Little information, however, is available about the role of IFN-γ in pulmonary LAM.

Our study shows that IFN-γ had little effect on TSC2-null ELT3 and LAMD cell growth. Although the mechanisms that cause cell resistance to antiproliferative and proapoptotic activities of IFN-γ are not fully established, some reports demonstrate that activation of STAT3, the positive regulator of cell proliferation and survival (Al Zaid Siddiquee and Turkson, 2008), prevents IFN-γ-dependent apoptosis (Sakamoto et al., 2005; Al Zaid Siddiquee and Turkson, 2008). STAT3 is a downstream effector of IFN-γ, but effects of IFN-γ on STAT3 activity seem to be cell type-dependent. Although IFN-γ activates STAT3 via JAK-dependent ^{Tyr705}STAT3 phosphorylation in different cell types (Sakamoto et al., 2005; Bai et al., 2008), it is also shown to inhibit STAT3 via ^{Tyr705}STAT3 dephosphorylation in TSC2-null MEFs (El-Hashemite et al., 2004) and human prostate cancer cells (Fang et al., 2006). Given that IFN-γ signaling is highly dependent on cell type, species, and stage of organism development (Platanias, 2005), the relationship between IFN-γ and STAT3 in LAM needs to be established.

Our data demonstrate that STAT3 is activated in LAM lungs and TSC2-null xenographic tumors in nude mice. STAT3 nuclear localization, ^{Tyr705}STAT3 phosphorylation,

Fig. 8. A and B, re-expression of TSC2 restores inhibitory effect of IFN-γ on cell proliferation. TSC2-null ELT3 (A) or LAMD (B) cells, transfected with plasmids expressing GFP-TSC2 or control GFP, were treated with 100 U/ml IFN-γ, rat or human, respectively, or diluent in the presence or absence of 10 ng/ml PDGF for 18 h, and then BrdU incorporation assay was performed. Data represent a percentage of GFP- and BrdU-positive cells per total number of GFP-positive cells. Data represent mean values + S.E. from two independent experiments. A, *, $p < 0.001$ for GFP-TSC2-transfected cells versus GFP-transfected cells; **, $p < 0.01$ for GFP-TSC2 + PDGF versus GFP + PDGF and GFP + IFN-γ + PDGF; ***, $p < 0.01$ for GFP-TSC2 + IFN-γ + PDGF versus GFP-TSC2 + PDGF. B, *, $p < 0.001$ for GFP-TSC2-transfected cells versus GFP-transfected cells; **, $p < 0.01$ for GFP-TSC2 + IFN-γ versus GFP-TSC2 and GFP + IFN-γ by ANOVA (Bonferroni-Dunn). C and D, TSC2 inhibits IFN-γ-dependent STAT3 phosphorylation in TSC2-null ELT3 and LAMD cells. TSC2-null ELT3 (C) or LAMD (D) cells, transfected with plasmids expressing GFP-tagged TSC2 (GFP-TSC2) or control GFP were serum-deprived for 24 h and then treated with 100 U/ml IFN-β, 100 U/ml IFN-γ, or diluent for 30 min followed by immunoblot analysis with anti-phospho-^{Tyr705}STAT3 and anti-STAT3 antibodies. Images are representative of two independent experiments (top). Dotted lines indicate the levels of DNA synthesis in GFP-TSC2-transfected cells treated with diluent. Quantitative analysis (bottom) was performed using Gel-Pro Analyzer software (Media Cybernetics, Inc., Bethesda, MD). Phospho-STAT3 optical density (OD) per total STAT3 OD in ELT3 (C) or LAMD (D) cells transfected with GFP was taken as one-fold. Data represent means + S.E. from two independent experiments by ANOVA (Bonferroni-Dunn).

and high STAT3 protein levels were detected in SM-like phospho-S6-positive cells of LAM lung and in the xenographic tumors. STAT3 participates in normal cellular events, such as differentiation, proliferation, and cell survival under cytokine, growth factor, and hormone signaling (Calò et al., 2003), and its expression is detected in normal cells and tissues, including airway and pulmonary vascular human SM cells (Simon et al., 2002; Bai et al., 2008) and human lungs (El-Hashemite and Kwiatkowski, 2005). However, both STAT3 expression and ^{Tyr705}STAT3 phosphorylation are persistently elevated in a variety of human tumors (Al Zaid Siddiquee and Turkson, 2008), which contributed to tumor cell growth and survival (Al Zaid Siddiquee and Turkson, 2008). Data from other laboratories also report increased phospho-^{Tyr705}STAT3 and total STAT3 levels in LAM lung compared with normal lung (El-Hashemite and Kwiatkowski, 2005) and in giant cells in tubers of the TSC patients (Baybis et al., 2004). Collectively, these data suggest that constitutive activation of mTOR as a result of TSC2 loss contributes to elevated STAT3 activity in vivo.

We demonstrated previously that loss of TSC2 function constitutively activates mTOR/S6K1 signaling and increases proliferation of human primary LAMD and TSC2-null rat ELT3 cells; and that re-expression of TSC2 or inhibition of mTOR activity by rapamycin markedly inhibits LAMD and TSC2-null ELT3 cell proliferation (Goncharova et al., 2002b, 2006a). mTOR activity is required for ^{Tyr705}STAT3 phosphorylation in monocytes, macrophages, and primary dendritic cells (Weichhart et al., 2008). In TSC2-null MEFs, mTOR inhibitor rapamycin induces ^{Tyr705}STAT3 dephosphorylation that correlates with inhibition of cell growth (El-Hashemite et al., 2004). In contrast, mTOR activation is required for IFN-γ-dependent ^{Tyr705}STAT3 dephosphorylation in human prostate cancer cells, and rapamycin protects STAT3 from dephosphorylation (Fang et al., 2006). Such variability in findings may be due to differential IFN-γ-dependent signaling in specific cell types (Platanias, 2005). However, the role of TSC2 and/or mTOR in regulating STAT3 protein levels and ^{Tyr705}STAT3 phosphorylation and its relevance to cell proliferation in LAM are not established. We found that either re-expression of TSC2 or rapamycin treatment inhibited IFNγ-dependent ^{Tyr705}STAT3 phosphorylation in TSC2-null and LAMD cells, demonstrating that TSC2 and mTOR modulate STAT3 activity. Rapamycin also synergized with IFN-γ in inhibiting cell proliferation but did not potentiate IFN-γ proapoptotic function, suggesting that rapamycin-dependent attenuation of STAT3 activity only partially restored IFN-γ functions. Synergistic effects of rapamycin and IFN-γ in inhibiting cell proliferation suggest that combination of lower doses of rapamycin and IFN-γ may attenuate side effects of each agent alone, which were used at higher doses. Future in vivo preclinical testing may determine whether combinational treatment at low doses of rapamycin and IFN-γ may provide a greater inhibitory effect on the TSC2-related tumor growth then each agent alone. Thus, combination of IFN-γ and rapamycin may be beneficial as potential therapy for LAM.

Although our data demonstrate that suppression of STAT3 activity is required for antiproliferative function of IFN-γ in LAMD and TSC2-null ELT3 cells, the exact mechanism by which IFN-γ inhibits cell proliferation in LAM is not fully understood. We found that in LAMD and TSC2-null ELT3 cells, IFN-γ simultaneously activates STAT1 (see Supplemental Figs. S2 and S3, respectively) and STAT3, which have opposing biological effects: STAT1 promotes antiproliferative and proapoptotic activities (Platanias, 2005) and STAT3 induces malignant transformation and tumorigenesis (Al Zaid Siddiquee and Turkson, 2008). Thus, the relative activation states of STAT1 and STAT3 by IFN-γ may regulate the final biological effects of IFN-γ on cell growth. Expression of IFN-γ receptor subunits (see Supplemental Fig. S1) and IFNγ-dependent STAT1 signaling were not altered in LAMD and TSC2-null ELT3 cells. Furthermore, re-expression of TSC2 or treatment with rapamycin, although inhibiting IFN-γ-dependent STAT3 activity, had little effect on IFN-γ-dependent activation of STAT1 (see Supplemental Fig. S3). Given the negative cross-regulation between STAT1 and STAT3 signaling (Qing and Stark, 2004), it is plausible that suppression of STAT3 activity by TSC2 or rapamycin or by direct inhibition of STAT3 is permissive for IFN-γ to inhibit growth and/or induce apoptosis via canonical STAT1 signaling pathway (Fig. 9).

Collectively, our current findings show that STAT3 was activated in vivo in LAM lungs and TSC2-null tumors in nude mice and in vitro in primary LAMD and TSC2-null cells. STAT3 activation was critical for increased proliferation and impeded antiproliferative and proapoptotic effects of IFN-γ in LAMD and TSC2-null ELT3 cells. Down-regulation of STAT3 protein levels or activity with specific siRNA or specific inhibitory peptide, respectively, markedly inhibited proliferation and induced apoptosis in TSC2-null ELT3 and LAMD cells and sensitized cells to growth-inhibitory and proapoptotic effects of IFN-γ. Re-expression of TSC2 or inhibition of mTOR by rapamycin inhibited ^{Tyr705}STAT3 phosphorylation and synergized with IFN-γ in inhibition of TSC2-null ELT3 and LAMD cell proliferation (Fig. 9). Although

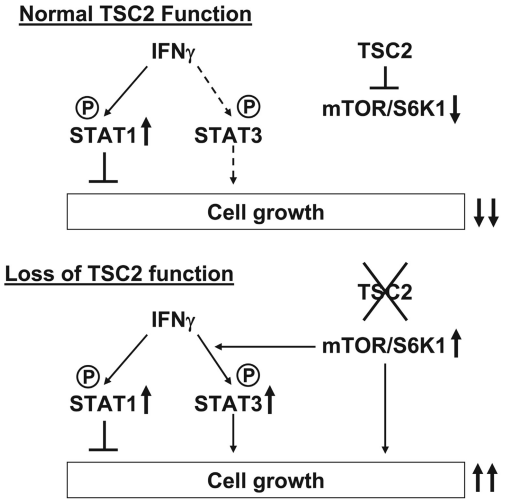

Fig. 9. Schematic representation of a potential mechanism of IFN-γ- and STAT3-dependent cell growth modulated by TSC2/mTOR signaling pathway. Top, in normal unstimulated cells, tumor suppressor TSC2 inhibits mTOR/S6K1 signaling pathway and cell proliferation. Treatment with IFN-γ activates canonical STAT1 signaling, induces modest phosphorylation of STAT3, and attenuates cell proliferation. Bottom, loss of TSC2 function leads to the constitutive activation of mTOR/S6K1 and increased STAT3 activity, which are both required for abnormal cell proliferation. IFN-γ induces STAT1 activation and increases STAT3 phosphorylation. Re-expression of TSC2 or inhibition of mTOR activity inhibits IFN-γ-dependent STAT3 phosphorylation and synergizes with IFN-γ in inhibition of cell proliferation.

IFN-γ did not markedly augment growth-inhibitory effects of rapamycin or TSC2 re-expression, in contrast, IFNγ alone had no effect on cell proliferation, suggesting that IFN-γ induces growth inhibition only then TSC2 function is restored by either TSC2 re-expression or inhibition of S6K1. This evidence leads us to conclusion that TSC2 loss of function impedes growth-inhibitory effects of IFN-γ, demonstrating biological significance of our findings. Collectively, our data suggest that STAT3 functions as a prosurvival molecule in LAM and suggest that STAT3 may be an attractive therapeutic target to inhibit abnormal LAM cell proliferation.

Acknowledgments

We thank the LAM Registry at the National Heart, Lung, and Blood Institute and the NDRI for providing LAM and bronchus tissue.

References

Agarwal C, Tyagi A, Kaur M, and Agarwal R (2007) Silibinin inhibits constitutive activation of Stat3, and causes caspase activation and apoptotic death of human prostate carcinoma DU145 cells. *Carcinogenesis* **28:**1463–1470.

Al Zaid Siddiquee K and Turkson J (2008) STAT3 as a target for inducing apoptosis in solid and hematological tumors. *Cell Res* **18:**254–267.

Bai Y, Ahmad U, Wang Y, Li JH, Choy JC, Kim RW, Kirkiles-Smith N, Maher SE, Karras JG, Bennett CF, et al. (2008) Interferon-γ induces X-linked inhibitor of apoptosis-associated factor-1 and Noxa expression and potentiates human vascular smooth muscle cell apoptosis by STAT3 activation. *J Biol Chem* **283:**6832–6842.

Baybis M, Yu J, Lee A, Golden JA, Weiner H, McKhann G 2nd, Aronica E, and Crino PB (2004) mTOR cascade activation distinguishes tubers from focal cortical dysplasia. *Ann Neurol* **56:**478–487.

Bissler JJ, McCormack FX, Young LR, Elwing JM, Chuck G, Leonard JM, Schmithorst VJ, Laor T, Brody AS, Bean J, et al. (2008) Sirolimus for angiomyolipoma in tuberous sclerosis complex or lymphangioleiomyomatosis. *N Engl J Med* **358:**140–151.

Calò V, Migliavacca M, Bazan V, Macaluso M, Buscemi M, Gebbia N, and Russo A (2003) STAT proteins: from normal control of cellular events to tumorigenesis. *J Cell Physiol* **197:**157–168.

Dabora SL, Roberts P, Nieto A, Perez R, Jozwiak S, Franz D, Bissler J, Thiele EA, Sims K, and Kwiatkowski DJ (2002) Association between a high-expressing interferon-gamma allele and a lower frequency of kidney angiomyolipomas in TSC2 patients. *Am J Hum Genet* **71:**750–758.

El-Hashemite N and Kwiatkowski DJ (2005) Interferon-gamma-Jak-Stat signaling in pulmonary lymphangioleiomyomatosis and renal angiomyolipoma: a potential therapeutic target. *Am J Respir Cell Mol Biol* **33:**227–230.

El-Hashemite N, Zhang H, Walker V, Hoffmeister KM, and Kwiatkowski DJ (2004) Perturbed IFN-gamma-Jak-signal transducers and activators of transcription signaling in tuberous sclerosis mouse models: synergistic effects of rapamycin-IFN-gamma treatment. *Cancer Res* **64:**3436–3443.

Fang P, Hwa V, and Rosenfeld RG (2006) Interferon-gamma-induced dephosphorylation of STAT3 and apoptosis are dependent on the mTOR pathway. *Exp Cell Res* **312:**1229–1239.

Goncharova EA, Ammit AJ, Irani C, Carroll RG, Eszterhas AJ, Panettieri RA, and Krymskaya VP (2002a) PI3K is required for proliferation and migration of human pulmonary vascular smooth muscle cells. *Am J Physiol Lung Cell Mol Physiol* **283:**L354–L363.

Goncharova EA and Krymskaya VP (2008) Pulmonary lymphangioleiomyomatosis (LAM): progress and current challenges. *J Cell Biochem* **103:**369–382.

Goncharova EA, Goncharov DA, Chisolm A, Spaits MS, Lim PN, Cesarone G, Khavin I, Tliba O, Amrani Y, Panettieri RA Jr, et al. (2008) Interferon β augments tuberous sclerosis complex 2 (TSC2)-dependent inhibition of TSC2-null ELT3 and human lymphangioleiomyomatosis-derived cell proliferation. *Mol Pharmacol* **73:**778–788.

Goncharova EA, Goncharov DA, Eszterhas A, Hunter DS, Glassberg MK, Yeung RS, Walker CL, Noonan D, Kwiatkowski DJ, Chou MM, et al. (2002b) Tuberin regulates p70 S6 kinase activation and ribosomal protein S6 phosphorylation. A role for the TSC2 tumor suppressor gene in pulmonary lymphangioleiomyomatosis (LAM). *J Biol Chem* **277:**30958–30967.

Goncharova EA, Goncharov DA, Spaits M, Noonan DJ, Talovskaya E, Eszterhas A, and Krymskaya VP (2006a) Abnormal smooth muscle cell growth in lymphangioleiomyomatosis: role for tumor suppressor TSC2. *Am J Respir Cell Mol Biol* **34:**561–572.

Goncharova EA, Lim P, Goncharov DA, Eszterhas A, Panettieri RA Jr, and Krymskaya VP (2006b) Assays for in vitro monitoring proliferation of human airway smooth muscle (ASM) and human pulmonary arterial vascular smooth muscle (VSM) cells. *Nat Protoc* **1:**2905–2908.

Gough DJ, Levy DE, Johnstone RW, and Clarke CJ (2008) IFNgamma signaling—does it mean JAK-STAT? *Cytokine Growth Factor Rev* **19:**383–394.

Hino O, Kobayashi T, and Mitani H (2002) Prevention of hereditary carcinogenesis. *Proc Jpn Acad* **78:**31–33.

Hino O, Kobayashi T, Momose S, Kikuchi Y, Adachi H, and Okimoto K (2003) Renal carcinogenesis: genotype, phenotype and dramatype. *Cancer Sci* **94:**142–147.

Howe SR, Gottardis MM, Everitt JI, Goldsworthy TL, Wolf DC, and Walker C (1995) Rodent model of reproductive tract leiomyomata. Establishment and characterization of tumor-derived cell lines. *Am J Pathol* **146:**1568–1579.

Kaur S, Lal L, Sassano A, Majchrzak-Kita B, Srikanth M, Baker DP, Petroulakis E, Hay N, Sonenberg N, Fish EN, et al. (2007) Regulatory effects of mammalian target of rapamycin-activated pathways in type I and II interferon signaling. *J Biol Chem* **282:**1757–1768.

Krymskaya VP and Goncharova EA (2009) PI3K/mTORC1 activation in hamartoma syndromes: therapeutic prospects. *Cell Cycle* **8:**403–413.

Lee L, Sudentas P, and Dabora SL (2006) Combination of a rapamycin analog (CCI-779) and interferon-gamma is more effective than single agents in treating a mouse model of tuberous sclerosis complex. *Genes Chromosomes Cancer* **45:**933–944.

Lee L, Sudentas P, Donohue B, Asrican K, Worku A, Walker V, Sun Y, Schmidt K, Albert MS, El-Hashemite N, et al. (2005) Efficacy of a rapamycin analog (CCI-779) and IFN-gamma in tuberous sclerosis mouse models. *Genes Chromosomes Cancer* **42:**213–227.

Lin L, Amin R, Gallicano GI, Glasgow E, Jogunoori W, Jessup JM, Zasloff M, Marshall JL, Shetty K, Johnson L, et al. (2009) The STAT3 inhibitor NSC 74859 is effective in hepatocellular cancers with disrupted TGF-beta signaling. *Oncogene* **28:**961–972.

Li Y, Inoki K, and Guan KL (2004) Biochemical and functional characterizations of small GTPase Rheb and TSC2 GAP activity. *Moll Cell Biol* **24:**7965–7975.

Messina MP, Rauktys A, Lee L, and Dabora SL (2007) Tuberous sclerosis preclinical studies: timing of treatment, combination of a rapamycin analog (CCI-779) and interferon-gamma, and comparison of rapamycin to CCI-779. *BMC Pharmacol* **7:**14.

Nguyen H, Ramana CV, Bayes J, and Stark GR (2001) Roles of phosphatidylinositol 3-kinase in interferon-γ-dependent phosphorylation of STAT1 on serine 727 and activation of gene expression. *J Biol Chem* **276:**33361–33368.

Ni CW, Hsieh HJ, Chao YJ, and Wang DL (2003) Shear flow attenuates serum-induced STAT3 activation in endothelial cells. *J Biol Chem* **278:**19702–19708.

Niu G, Heller R, Catlett-Falcone R, Coppola D, Jaroszeski M, Dalton W, Jove R, and Yu H (1999) Gene therapy with dominant-negative Stat3 suppresses growth of the murine melanoma B16 tumor in vivo. *Cancer Res* **59:**5059–5063.

Platanias LC (2005) Mechanisms of type-I- and type-II-interferon-mediated signalling. *Nat Rev Immunol* **5:**375–386.

Qing Y and Stark GR (2004) Alternative activation of STAT1 and STAT3 in response to interferon-γ. *J Biol Chem* **279:**41679–41685.

Riemenschneider MJ, Betensky RA, Pasedag SM, and Louis DN (2006) AKT activation in human glioblastomas enhances proliferation via TSC2 and S6 kinase signaling. *Cancer Res* **66:**5618–5622.

Sabatini DM (2006) mTOR and cancer: insights into a complex relationship. *Nat Rev Cancer* **6:**729–734.

Sakamoto E, Hato F, Kato T, Sakamoto C, Akahori M, Hino M, and Kitagawa S (2005) Type I and type II interferons delay human neutrophil apoptosis via activation of STAT3 and up-regulation of cellular inhibitor of apoptosis 2. *J Leukoc Biol* **78:**301–309.

Simon AR, Takahashi S, Severgnini M, Fanburg BL, and Cochran BH (2002) Role of the JAK-STAT pathway in PDGF-stimulated proliferation of human airway smooth muscle cells. *Am J Physiol Lung Cell Mol Physiol* **282:**L1296–L1304.

Turkson J, Ryan D, Kim JS, Zhang Y, Chen Z, Haura E, Laudano A, Sebti S, Hamilton AD, and Jove R (2001) Phosphotyrosyl peptides block Stat3-mediated DNA binding activity, gene regulation, and cell transformation. *J Biol Chem* **276:**45443–45455.

Weichhart T, Costantino G, Poglitsch M, Rosner M, Zeyda M, Stuhlmeier KM, Kolbe T, Stulnig TM, Hörl WH, Hengstschläger M, et al. (2008) The TSC-mTOR signaling pathway regulates the innate inflammatory response. *Immunity* **29:**565–577.

Yoshiura S, Ohtsuka T, Takenaka Y, Nagahara H, Yoshikawa K, and Kageyama R (2007) Ultradian oscillations of Stat, Smad, and Hes1 expression in response to serum. *Proc Natl Acad Sci U S A* **104:**11292–11297.

Zhou J, Wulfkuhle J, Zhang H, Gu P, Yang Y, Deng J, Margolick JB, Liotta LA, Petricoin E 3rd, and Zhang Y (2007) Activation of the PTEN/mTOR/STAT3 pathway in breast cancer stem-like cells is required for viability and maintenance. *Proc Natl Acad Sci U S A* **104:**16158–16163.

Address correspondence to: Dr. Elena A. Goncharova, Department of Medicine, University of Pennsylvania, TRL, Room 1214 , 125 South 31st St., Philadelphia, PA 19104. E-mail: goncharo@mail.med.upenn.edu